Journal of Cellular Biochemistry 93:133–141 (2004)

Increased Apoptosis of Periprostatic Adipose Tissue in VDR Null Mice

Meral Guzey,[1] Drazen Jukic,[2] Julie Arlotti,[1] Marie Acquafondata,[2] Rajiv Dhir,[2] and Robert H. Getzenberg[1,2,3,4]*

[1]Department of Urology, University of Pittsburgh, Pittsburgh, Pennsylvania
[2]Department of Pathology, University of Pittsburgh, Pittsburgh, Pennsylvania
[3]Department of Pharmacology, University of Pittsburgh, Pittsburgh, Pennsylvania
[4]University of Pittsburgh Cancer Institute, University of Pittsburgh, Pittsburgh, Pennsylvania

Abstract The vitamin D receptor (VDR) is a member of the steroid/retinoid receptor superfamily of nuclear receptors that controls mineral ion homeostatis and has potential tumor-suppressive functions for various cancer types, specifically prostate cancer. A VDR ablated transgenic animal model (VDDRII, vitamin D-dependent rickets type II) has been developed and the animals typically have various diseases including, hypocalcemia, hyperparathyroidism, rickets, osteomalacia, and alopecia. This transgenic mouse system provides us with a model to decipher the influences of the VDR on prostatic growth and function. VDRs are abundant both in prostatic epithelial and stromal cells, and vitamin D signaling can be studied in this model. Although, there were no gross differences between the prostate tissue of the experimental and control groups, VDR null mice showed fat necrosis and individual cell apoptosis in the periprostatic adipose tissue. This indicates a possible role of VDR in the signaling pathways resulting the prostate. This may be particularly attractive for VDR targets for the inhibition of cancer progression using VD_3 and its analogs as potential chemo-preventive agents. J. Cell. Biochem. 93: 133–141, 2004.

Key words: prostate gland; VDR; vitamin D_3; apoptosis; VDR-knock out mice

The physiological actions of VD_3 are mediated at least in part by the vitamin D receptor (VDR) [Haussler et al., 1998]. This predominantly nuclear protein is a member of the steroid receptor family of transcription factors and functions like other nuclear receptors to regulate the expression of genes involved in a wide variety of cellular activities. The major role of VD_3 is to maintain calcium and phosphorous homeostasis through its direct actions on gene expression in the intestine, kidney, and bone [Jones et al., 1998]. Ligand association with the VDR leads to rapid activation and subsequent accumulation of the receptor on vitamin D response elements (VDREs) located within the promoter regions of specific genes [Haussler et al., 1998]. VDRE binding is facilitated by the retinoid X receptor (RXR) that functions as a heterodimeric DNA binding partner as well as a participant in transactivation [Thompson et al., 2001].

Growth suppressive effects of VDR ligands on epithelial cancer cells in vitro have prompted interest in the possibility of applying natural or synthetic VDR ligands for the treatment of cancer [van Leeuwen and Pols, 1997]. Prostate cancer is among the types of tumor cells with documented sensitivity to VDR ligands. VD_3 and its less calcemic synthetic analogues have been shown to inhibit in vitro growth of established human prostate carcinoma cell lines and primary cultures of normal and prostate cancer cells [Ly et al., 1999; Zhao et al., 1999]. Depending on the particular cell line tested, VDR ligands can induce cell cycle arrest, differentiation, apoptosis, or combinations of these events [Guzey and DeLuca, 1997]. Functional VDR is necessary for the growth-inhibitory effect of VDR. However, prostate cancer cell

*Correspondence to: Robert H. Getzenberg, PhD, Shadyside Medical Center, 5200 Centre Ave., Suite G42, Pittsburgh, PA 15232. E-mail: getzenbergrh@upmc.edu

Received 26 April 2004; Accepted 28 April 2004
DOI 10.1002/jcb.20172
Published online 28 June 2004 in Wiley InterScience (www.interscience.wiley.com).

lines vary in their sensitivity to VD_3 and its synthetic analogues in ways that cannot be explained by differences in VDR protein levels or rates of ligand metabolism, suggesting the existence of mechanisms for modulating VDR function post-ligand binding. This variability in bioresponses to synthetic VD_3 analogues has also been observed in vivo in clinical trials involving men with advanced prostate cancer [Gross et al., 1997].

In these studies, we have utilized the VDR null (−/−) mouse [Li et al., 1997] to provide evidence of a role for the VDR in protection against prostate cancer development. Targeting disruption of the second zinc finger of the VDR gene in mice, led to the development of a transgenic animal model [Li et al., 1997], that has been order to study vitamin D signaling in the prostate gland. The phenotype is identical to that of the human VDDRII. Animals developed progressive alopecia, necrotic, and apoptotic lesions in periprostatic adipose tissue. We observe no abnormalities in the prostate glands of the VDR null mice compared to their controls. However, we find that VDR (−/−) mice (but not the VDR +/+ control mice) develop apoptosis and necrosis in the periprostatic adipose tissue. These data provide the first in vivo evidence for the VDR effects on apoptotic signaling events in and around the prostate gland.

MATERIALS AND METHODS

Animal Maintenance

A breeding colony of VDR knockout mice was established from mice generously provided by Dr. Marie Demay (Harvard Medical School, Boston, MA). They were maintained in a virus-free and parasite-free barrier facility and exposed to a 12 h light, 12 h dark cycle. The mice were maintained in cages with wooden shavings and consumed distilled water and non-purified or purified diet ab libitum. All experimental protocols were received and approved by Institutional Animal Care and Use Committee (IACUC, University of Pittsburgh-Pittsburgh, PA).

PCR

The VDR null mutant mice used in this study were produced by heterozygous breeding pairs. When the pups were 10–14 days old, they were ear-tagged and their tails were snipped. Tails were agitated overnight at 55°C in lysis buffer (1 M Tris, pH 8.5; 5 M NaCl, 0.5 M EDTA, 10% SDS) and 500 μg proteinase K. The following day an equal volume of phenol:chloroform was added and the tubes were centrifuged at 15,800*g*. The aqueous layer was retained and 2.5× volume of cold absolute ethanol was used to precipitate the DNA. The DNA strands were dissolved in TE (1 M Tris, pH 8; 0.5 M EDTA, pH 8).

The isolated DNA was then subjected to PCR screening using a PTC-100 Programmable Thermal Control PCR machine (MJ Research, Inc., Watertown, MA). Two separate reactions were performed under the following conditions: *NEO3*: GCT GCT CTG ATG CCG CCG TGT TC; *NEO4*: GCA CTT CGC CCA ATA GCA GCC AG. An initial denaturation of 5 min at 94°C was followed by 36 cycles of 1 min at 94°C, 1 min of annealing at 61°C, and 1 min of extension at 72°C. This amplification produced a 200 bp fragment. *MR5:* CTG CCC TGC TCC ACA GTC CTT. *MR6:* GCA GAC TCT CCA ATG TGA AGC. An initial denaturation of 5 min at 94°C was followed by 27 cycles of 1 min at 94°C, 1 min of annealing at 65°C, and 1 min of extension at 72°C. The final step was 7 min at 72°C. This amplification generated an 800 bp fragment.

In both cases, each reaction contained 1 μg DNA, 2 μM of each primer (Invitrogen, Carlsbad, CA), 0.2 mM dNTP mix (Gibco, Rockville, MD), 10× Taq buffer, 3 mM $MgCl_2$, and 0.5 U Taq DNA polymerase (Promega, Madison, WI) in a final volume of 50 μl. The completed reactions were run at 100 V on a 2% Nu-Sieve agarose gel (BioWhitaker, Walkersville, MD).

Immunohistochemistry

Histological examinations (H&E) were stained using the immunohistochemical ABC method. Briefly, formalin-fixed prostates were embedded in paraffin, sectioned at 4 μM, and stained with H&E for routine histological assessment. A pathologist with experience both in human and murine genitourinary systems interpreted the slides for the presence of any abnormalities.

Antibodies and Immunoblotting

Tissue lysates were prepared using RIPA buffer (10 mM Tris, [pH: 7.4], 150 mM NaCl, 1% Triton ×100, 1% Na-deoxycholate, 0.1% SDS, 5mM EDTA), and alternatively high-salt buffer [20 mM HEPES (pH 7.9), 20 mM NaF, 1 mM $Na_3P_2O_7$, 1 mM Na_3VO_4, 1 mM EDTA, 1 mM EGTA, 1 mM DTT, 0.5 mM phenylmethylsulfonyl

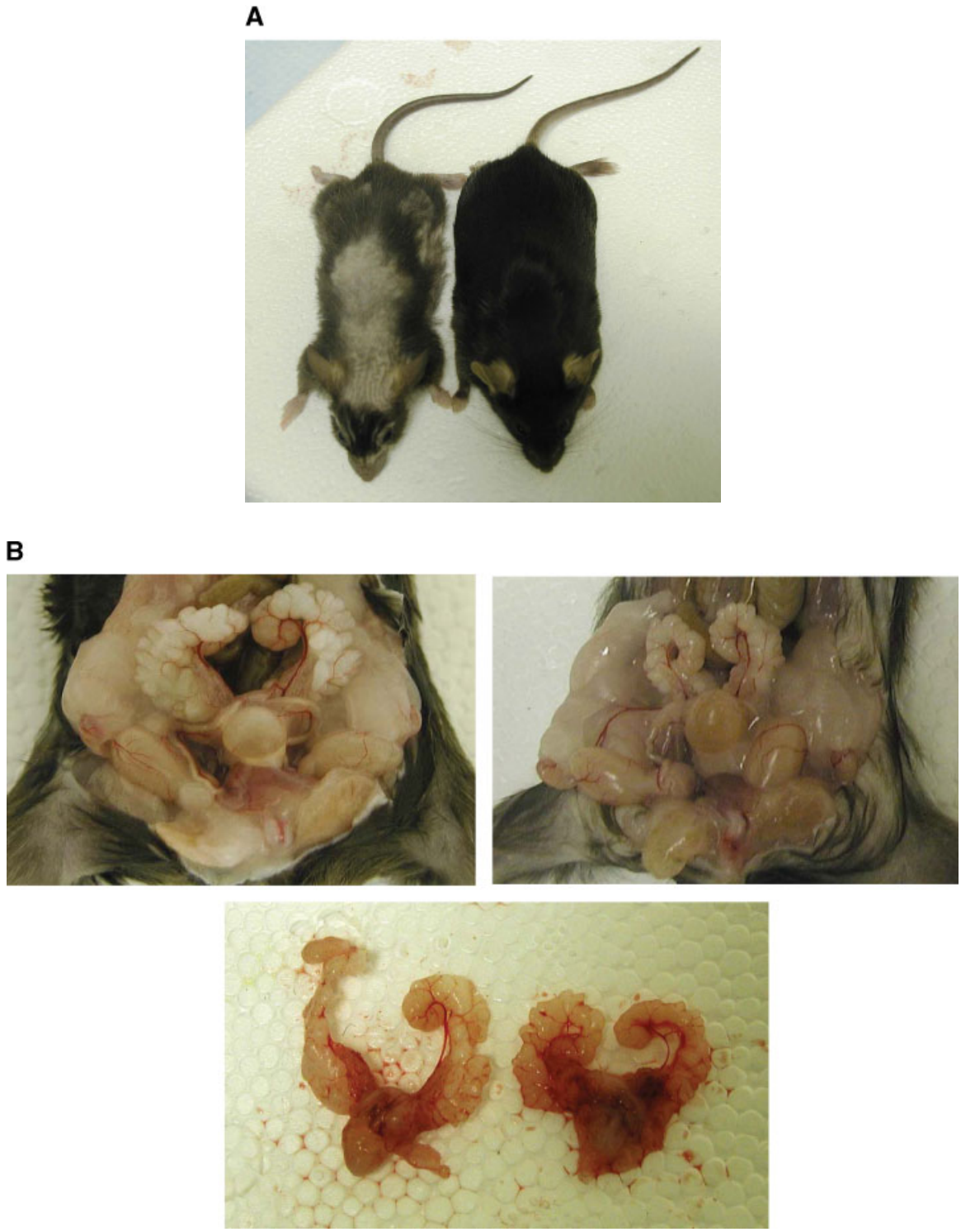

Fig. 1. **A**: Appearance of VDR ablated male mice 3.5 months of age. The genotypes of the mice, from left to right, are heterozygotes, and wild type control murines. **B**: Prostates of wild type (**left**) and VDR null mice (**right**). There was no tumor mass found in urinary bladder, seminal vesicles, or at prostate tissue. However, there were necrosis and apoptosis in the periprostatic adipose tissue. [Color figure can be viewed in the online issue, which is available at www.interscience.wiley.com.]

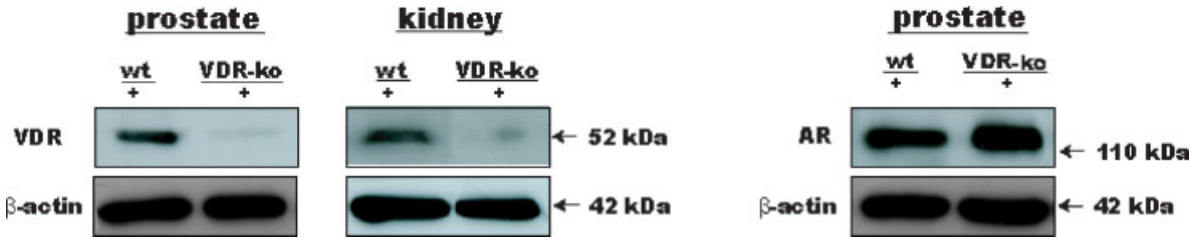

Fig. 2. VDR and AR protein expression levels in prostate and kidney tissues in VDR null mice. AR protein expression level stayed the same at prostate tissues both in VDR null and wild type murines, while VDR expression was not detectable as expected in VDR null mice. [Color figure can be viewed in the online issue, which is available at www.interscience.wiley.com.]

fluoride, 420 mM NaCl, 20% glycerol, 1 μg/ml leupeptin, and 1 μg/ml aprotinin], followed by snap-freezing in ethanol/dry ice for 5 min and thawing on ice for 10 min. The freeze and thaw procedures were repeated again for a total of two times. The samples were normalized for total protein content (25 μg of protein), and subjected to SDS–PAGE using 8–12% gels, followed by electro-transfer to 0.45 μm nitrocellulose transfer membranes (Bio-Rad, Hercules, CA). Blots were incubated as described [Harlow and Lane, 1999] with primary antibodies, including 1/500 (v:v) mouse VDR monoclonal antibody (Santa Cruz, CA), 1/1,000 (v:v) mouse AR monoclonal antibody (Santa Cruz, CA), 1/10,000 (v:v) mouse monoclonal anti-β-actin, clone AC-74 mouse ascites fluid (Sigma, Saint Louis, Missouri). Immuno-detection was accomplished using horseradish peroxidase-conjugated secondary antibodies (Biorad, Hercules, CA) and an enhanced chemiluminescence detection method (ECL) (Amersham/Pharmacia Biotech.) with exposure to X-ray film (XAR, Eastman Kodak, Co., Rochester, NY).

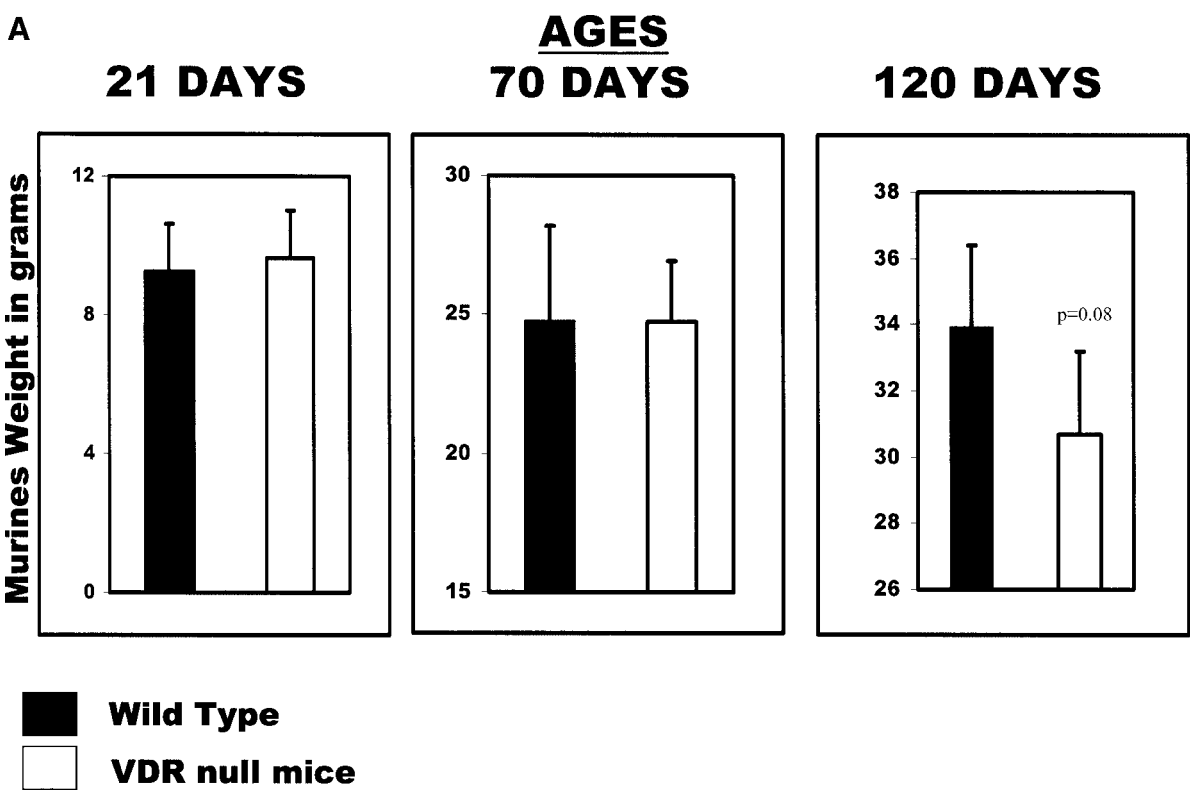

Fig. 3. There were at least six animals for each of the three different, 21, 70, and 120 days time points. These time points were selected based upon the hormonal stages of development (prepuberty, post puberty, and adult). **A**: Shows the total weight of these animals against the control groups, lung, prostate, seminal vesicle, and bladder weights (±SD).

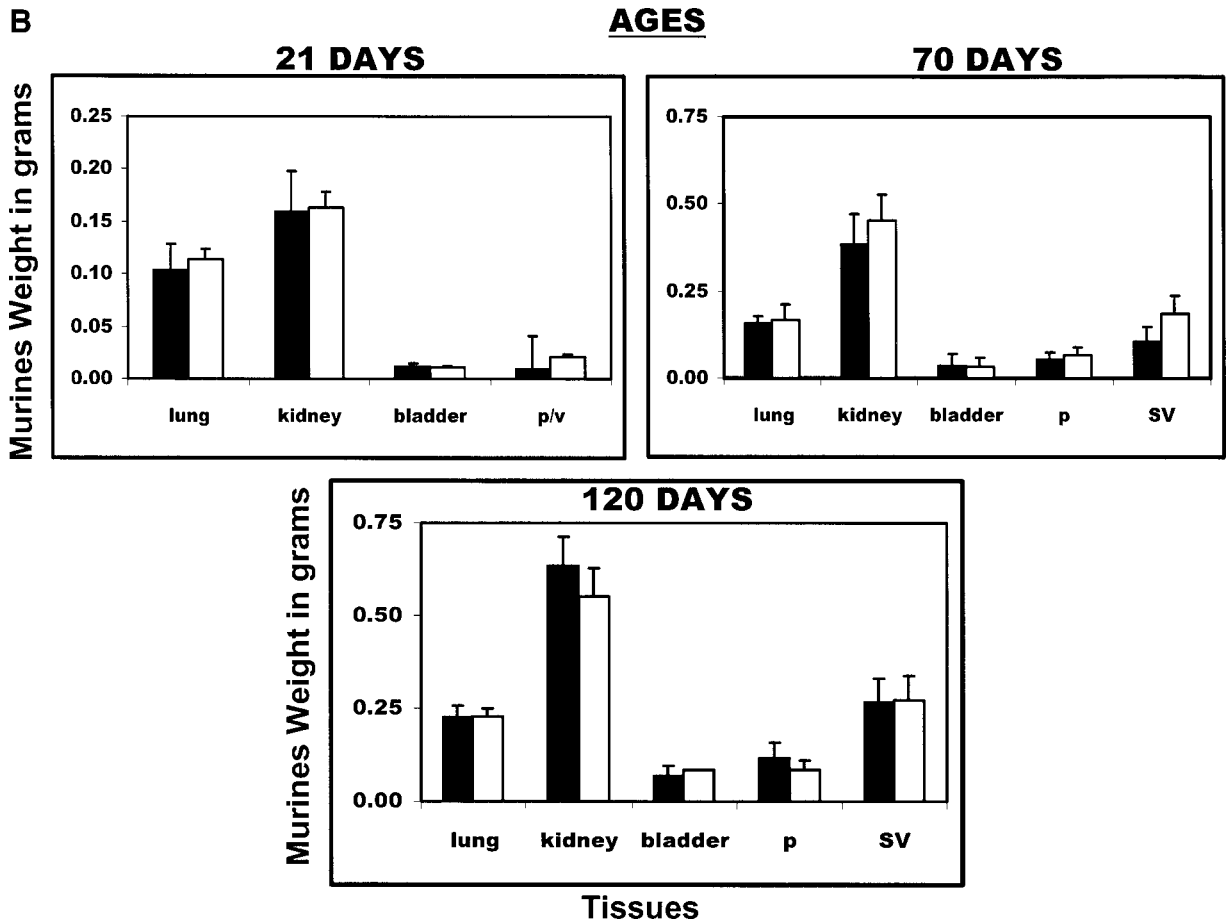

Fig. 3. (*Continued*)

Assessment of Apoptosis

Paraffin-embedded formalin fixed tissue sections were analyzed for DNA fragmentation using the TUNEL fluorescence labeling kit from Chemicon (Temecula, CA), following the instructions provided by the manufacturer. The 4 μm tissue sections were stained using the immunohistochemical ABC method, and analyzed by microscopy. The tissues were then evaluated for expression of nuclear staining and cells were counted in each section, on the semiquantitative scale (from 0 to 3). The percentages of cells staining for each point of the scale were reported, giving a comprehensive staining overview.

TABLE I. Differentiation Grades

Ages of the murines (days)	21	70	120
Differentiation[a]	5	5	3 and 4

[a]Grade 1:—least differentiated, Grade 6:—most differentiated.

Statistical Methods and Analysis

All experiments were performed in triplicate and mean values were presented as ±standard error. Data were analyzed by a Student's *t*-test, and means were considered significantly different if $P < 0.05$. The software used for these analyses was Graph Pad InStat, V2.02.

RESULTS

VDR null (−/−) mice were generated by deleting a 5-kb fragment of genomic DNA encoding the second zinc finger of the receptor DNA-binding domain [Li et al., 1997]. At the age of 70 days, the VDR-null mice developed alopecia as reported previously [Li et al., 1997; Kearns and Demay, 2000]. As shown in Figure 1A, this hair loss progressed to involve the entire body over the 120 days. However there were neither gross nor microscopic abnormalities observed in the prostate gland of the VDR null mice (Fig. 1B).

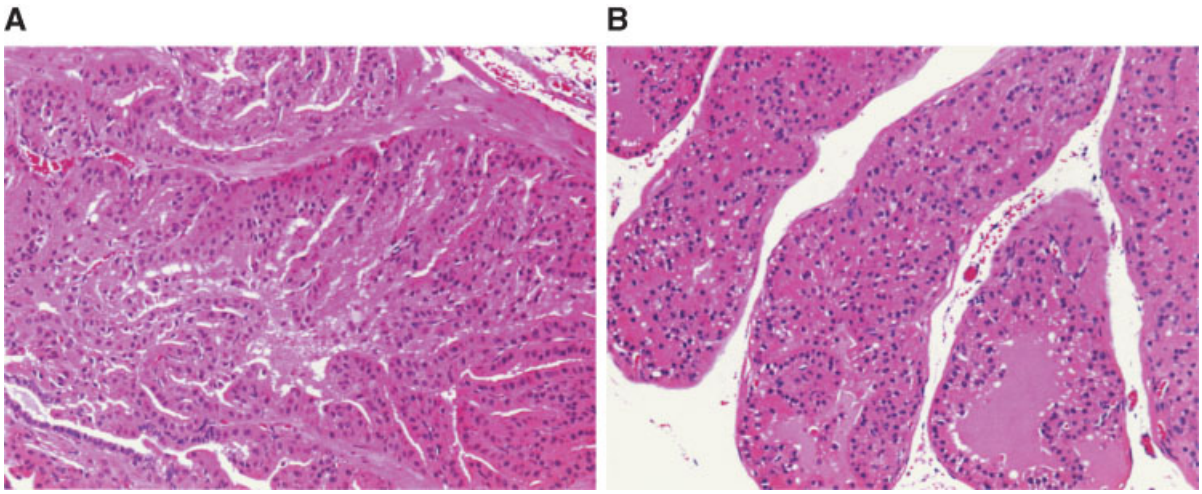

Fig. 4. Hematoxilin and eosin staining of the prostate from a 120-days old wild type (**A**) and a VDR null mice (**B**).

To investigate transgenesis on newly breeding mice RT-PCR analyses were conducted as described in the Materials and Methods. Tissues collected from prostates and alternatively from kidneys were examined for VDR expression. We observed a specific band representing VDR for the control animals, which as expected was absent in the transgenic animals. However, AR expression level did not change between control to transgenic animals (Fig. 2).

The −/− animals were indistinguishable from their +/+ and +/− littermates at birth and first 21 days; however, from 70 days of age, they failed to grow as rapidly as their +/+ and +/− littermates and weighed 7% less by 120 days ($P = 0.08$) (Fig. 3A and B). There were no weight differences between selected tissues of 21 and 70 days old animals. For example, the 120 days prostates were smaller in the transgenic mice but the statistical analyses showed no significance between the two groups (Fig. 3B).

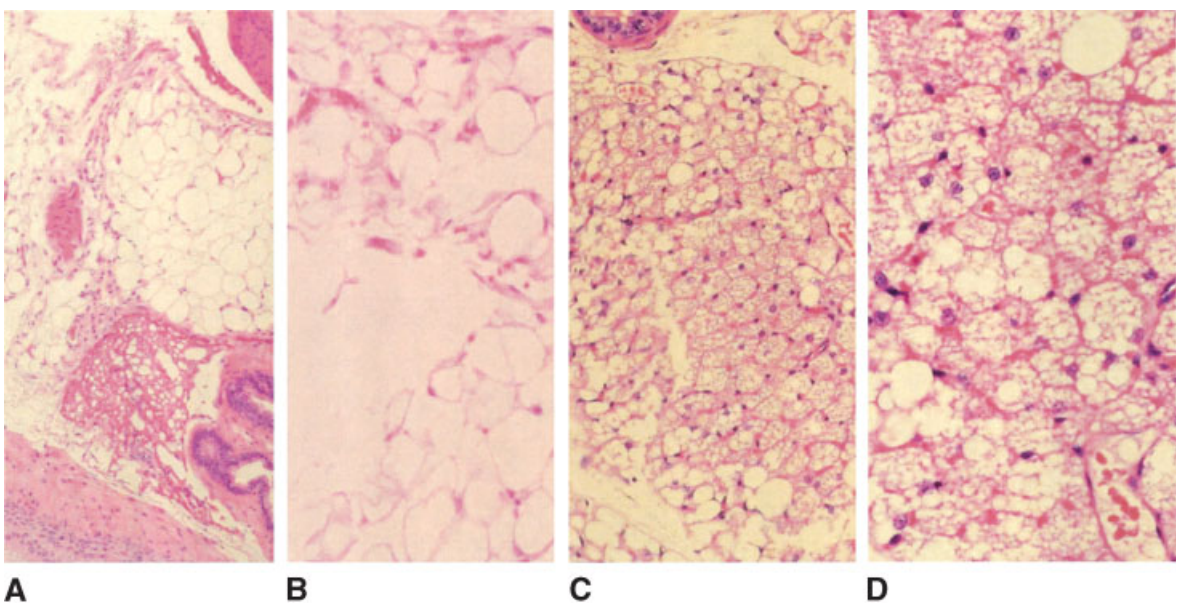

Fig. 5. This composite image reveals similarities and differences in periprostatic adipose tissue between wild type mice (**A** and **B**) and knock-out mice (**C** and **D**). Image A (10×, H/E) reveals usual periprostatic fat distribution as seen in healthy wild type mice; the cellular detail is preserved (B—20×, H/E), and adipocytes have the usual signet-ring cell appearance. Image C (10×, H/E) is taken from knockout mice; higher power of the same area (Image D—20× H/E) reveals partially necrotic adipocytes, with eosinophilic cytoplasm, microvesicular change, and prominent nuclei.

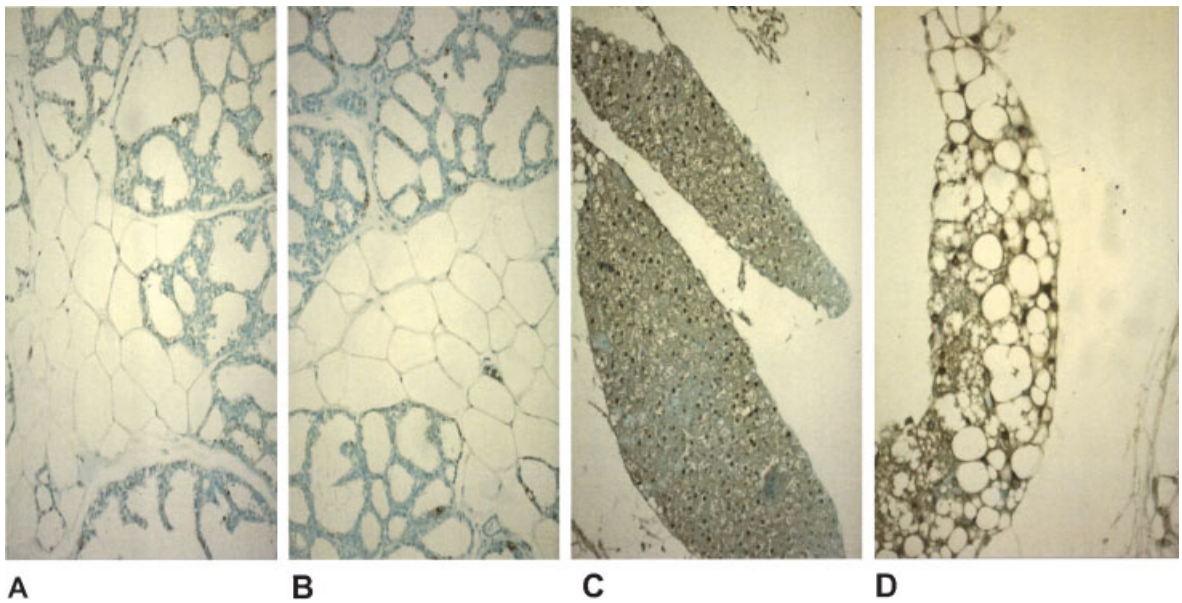

Fig. 6. **A** and **B** panels represent prostate and periprostatic fat in wild type mice; one can observe preserved architecture with focal expression of APOPTAG antibody in nuclei of prostatic gland and negligible positivity in the fat (adipocytes). In **Panel C**, one sees periprostatic fat with apoptotic bodies and microvacuolated cytoplasm, in which ~60% of adipocytes strongly express APOPTAG. This is exemplified in the **Panel D**—high power.

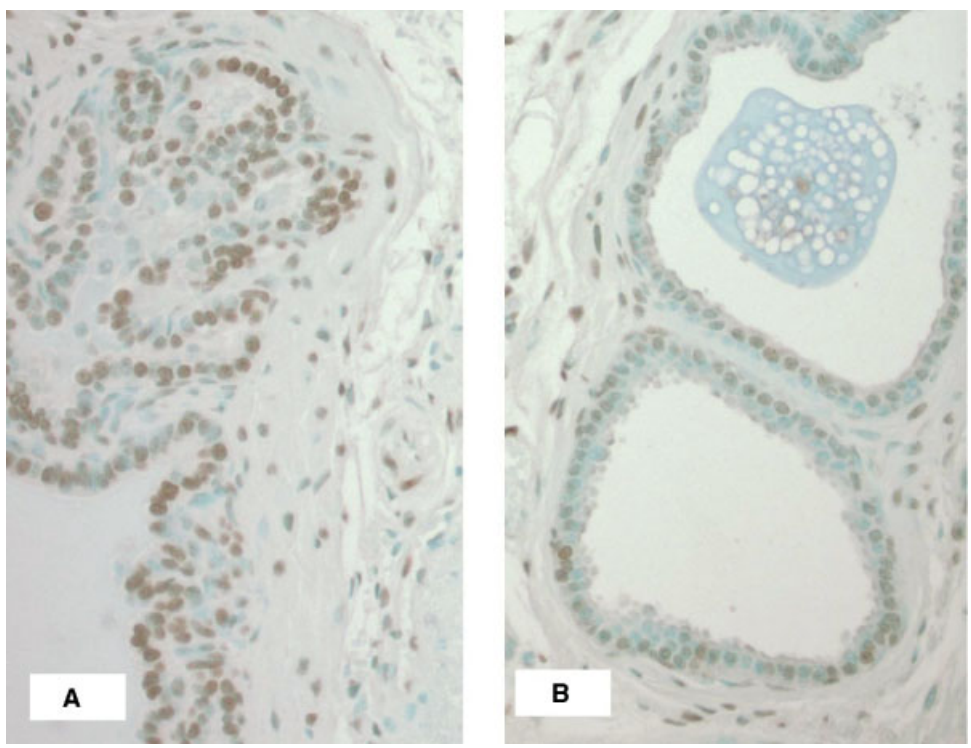

Fig. 7. DNA fragmentation was analyzed by using the TUNEL fluorescence labeling kit from Chemicon (Temecula, CA), following the instructions provided by the manufacturer on the tissue from VDR-KO-mice (**A**) versus Control-WT (**B**).

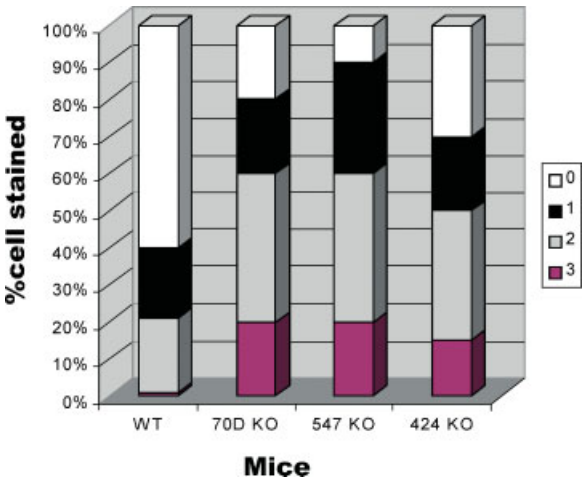

Fig. 8. In essence, we have utilized the Apoptosis detection Kit S7101. The tissues were evaluated for expression of nuclear staining and cells were counted in each section, on the semiquantitative scale (from 0 to 3). The percentages of cells staining for each point of the scale were reported, giving a comprehensive staining overview.

Microscopic examination of hematoxylin–eosin (H&E)-stained sections of prostates from the animals at 21, 70, and 120 days showed no major histological differences (Table I) in comparison to controls [Fig. 4A,B (control) (transgenic mice)]. Although there were no apparent abnormalities in the prostate glands of the VDR null male mice, there were areas of apoptotis and fat necrosis in the microscopic evaluation of the periprostatic adipose tissue (Fig. 5). In order to confirm the presence of apoptotic cells, DNA damage was visualized using a TUNEL assay kit (Fig. 6A,B,C,D Control animals, KO mice). Further, tissue sections were evaluated for their amount of staining intensity 1 through 3. This scaling was 1 as least apoptotic, 3 most apoptotic and zero without any response to Apoptag-TUNEL staining (Figs. 7A,B and 8). Our results indicated that 12% more of the null mice were in +3, however the control animals were 45% more in 0 level of staining out of six animal tissues of each group (Fig. 8).

DISCUSSION

The discovery of the presence of VDRs within the epithelial cells of the prostate [Miller et al., 1992] led to the hypothesis that VD_3 might play a direct role in prostate biology. VDR abundance in primary cultures of the prostatic cancer cells spans a wide range, but overall does not differ significantly from normal cells [Peehl et al., 1994]. The importance of vitamin D signaling for prostate carcinoma is well recognized. We show for the first time in this study that in the absence of VDR, necrosis and apoptosis eventually develop in the periprostatic adipose tissue of mice. We do not know which molecular mediators of apoptosis are activated in the absence of VDR, but selectivity of this effect suggests that VD_3 plays metabolic cues that maintain adipose cell survival.

VDR null mutant mice are fertile if they are fed an appropriate diet [Johnson and DeLuca, 2001]. Further, they are able to lactate, indicating that mammary gland function also is not overtly affected [Zinser et al., 2002]. This was confirmed by normal ductal morphogenesis and branching compared to WT animals [Guzey et al., 2002; Welsh et al., 2003]. We likewise did not detect any major differences in the architecture of prostate gland between the previously normal and VDR null mice.

The functional importance of VDRs in cancer through apoptotic signaling is beginning to be clarified [Blutt et al., 2000; Guzey et al., 2002]. Our data indicate that prostate glands from VDR-null murines exhibit apoptosis and necrosis in the peri-prostatic adipose tissue as compared with wild type animal. This finding suggests that VDR plays an important role in apoptotic signaling. These results support our previous finding in vitro that VDR could play a key role for a group of apoptotic and anti-apoptotic genes. Future investigation is necessary to evaluate gene expression profiling, to determine for the genes that play control roles in this cellular signaling pathway. Additionally, new transcriptional targets of the VDR will be identified which are involved in prostate gland proliferation, differentiation and apoptosis. As a conclusion this will help us to define attractive targets for the inhibition of cancer progression using potential chemo preventive agents or further to provide initial information for new drug discovery in the field.

ACKNOWLEDGMENTS

We thank Marianne Natoru and Jason D'Amato for their technical support.

REFERENCES

Blutt SE, McDonnell TJ, Polek TC, Weigel NL. 2000. Calcitriol-induced apoptosis in LNCaP cells is blocked by overexpression of Bcl-2. Endocrinology 141:10–17.

Gross C, Peehl DM, Feldman D. 1997. Vitamin D and prostate cancer. In: Feldman D, Glorieux FH, Pike WP, editors. Vitamin D. San Diego: Academic Press. pp 1125–1200.

Guzey M, DeLuca HF. 1997. A group of deltanoids (vitamin D analogs) regulate cell growth and proliferation in small cell carcinoma cell lines. Res Commun Mol Pathol Pharmacol 98:3–18.

Guzey M, Kitada S, Reed JC. 2002. Apoptosis induction by 1alpha, 25-dihydroxyvitamin D_3 in prostate cancer. Mol Cancer Ther 1:667–677.

Harlow E, Lane D. 1999. Immunoblotting. In: Using antibodies. New York: Cold Spring Harbor Laboratories, INC. 267–309.

Haussler MR, Whitfield GK, Haussler CA, Hsieh JC, Thompson PD, Selznick SH, Dominguez CE, Jurutka PW. 1998. The nuclear vitamin D receptor: Biological and molecular regulatory properties revealed. J Bone Miner Res 13:325–349.

Johnson LE, DeLuca HF. 2001. Vitamin D receptor null mutant mice fed high levels of calcium are fertile. J Nutr 131:1787–1791.

Jones G, Strugnell SA, DeLuca HF. 1998. Current understanding of the molecular actions of vitamin D. Physiol Rev 78:1193–1231.

Kearns AE, Demay MB. 2000. BMP-2 induces the expression of activin betaA and follistatin in vitro. J Cell Biochem 79:80–88.

Li YC, Pirro AE, Amling M, Delling G, Baron R, Bronson R, Demay MB. 1997. Targeted ablation of the vitamin D receptor: An animal model of vitamin D-dependent rickets type II with alopecia. Proc Natl Acad Sci USA 94:9831–9835.

Ly LH, Zhao XY, Holloway L, Feldman D. 1999. Liarozole acts synergistically with 1alpha, 25-dihydroxyvitamin D3 to inhibit growth of DU-145 human prostate cancer cells by blocking 24-hydroxylase activity. Endocrinology 140:2071–2079.

Miller GJ, Stapleton GE, Ferrara JA, Lucia MS, Pfister S, Hedlund TE, Upadhya P. 1992. The human prostatic carcinoma cell line LNCaP expresses biologically active, specific receptors for 1 alpha, 25-dihydroxyvitamin D3. Cancer Res 52:515–520.

Peehl DM, Skowronski RJ, Leung GK, Wong ST, Stamey TA, Feldman D. 1994. Antiproliferative effects of 1,25-dihydroxyvitamin D_3 on primary cultures of human prostatic cells. Cancer Res 54:805–810.

Thompson PD, Remus LS, Hsieh JC, Jurutka PW, Whitfield GK, Galligan MA, Encinas DC, Haussler CA, Haussler MR. 2001. Distinct retinoid X receptor activation function-2 residues mediate transactivation in homodimeric and vitamin D receptor heterodimeric contexts. J Mol Endocrinol 27:211–227.

van Leeuwen JPTM, Pols HAP. 1997. Anticancer and differentiation. In: Feldman D, Glorieuex FH, Pike JW, editors. Vitamin D. San Diego, CA: Academic Press. pp 1089–1105.

Welsh J, Wietzke JA, Zinser GM, Byrne B, Smith K, Narvaez CJ. 2003. Vitamin D-3 receptor as a target for breast cancer prevention. J Nutr 133:2425S–2433S.

Zhao XY, Ly LH, Peehl DM, Feldman D. 1999. Induction of androgen receptor by 1alpha, 25-dihydroxyvitamin D_3 and 9-*cis* retinoic acid in LNCaP human prostate cancer cells. Endocrinology 140:1205–1212.

Zinser G, Packman K, Welsh J. 2002. Vitamin D(3) receptor ablation alters mammary gland morphogenesis. Development 129:3067–3076.